Chemical Kinetic Modeling Study of the Effects of Oxygenated Hydrocarbons on Soot Emissions from Diesel Engines†

Charles K. Westbrook,* William J. Pitz, and Henry J. Curran‡

Lawrence Livermore National Laboratory, P.O. Box 808, Livermore, California 94550

Received: November 3, 2005; In Final Form: March 3, 2006

A detailed chemical kinetic modeling approach is used to examine the phenomenon of suppression of sooting in diesel engines by the addition of oxygenated hydrocarbon species to the fuel. This suppression, which has been observed experimentally for a few years, is explained kinetically as a reduction in concentrations of soot precursors present in the hot products of a fuel-rich diesel ignition zone when oxygenates are included. The kinetic model is also used to show how different oxygenates, ester structures in particular, can have different soot-suppression efficiencies due to differences in the molecular structure of the oxygenated species.

Introduction

Soot emissions from diesel engines continue to be a serious environmental concern. While significant reductions have been achieved in recent years, legislated limits are being steadily tightened[1] and further improvements will require a much more fundamental understanding of soot production and evolution to meet these regulations. Many experimental, theoretical, and computer modeling studies have been devoted to these problems to refine our understanding of the reaction pathways producing and consuming soot in engines and flames. Attention has been given to the fact that different hydrocarbon fuels can produce significantly different quantities of soot[2] and that modifications of soot-producing fuels can lead to considerable reductions in soot emission. In particular, the use of oxygenated fuels and fuel additives has demonstrated the potential to reduce soot emissions from diesel engines.

In a recent experimental study, Miyamoto et al.[3] found that soot emissions from diesel engines were reduced when oxygenated hydrocarbons were blended with the regular diesel fuel. The amount of soot reduction depended on the total amount of oxygen added to the diesel fuel, and each of the oxygenated species added to the fuel (di-*n*-butyl ether, ethylhexyl acetate, ethylene glycol mono-*n*-butyl ether, and diethylene glycol dimethyl ether) had approximately the same effectiveness in reducing soot emissions when measured in terms of the amount of oxygen added to the fuel. With each additive, soot emissions declined steadily as the additive concentration increased, and by the time the oxygen content of the fuel reached 25−30% by mass, virtually all soot emissions had disappeared, as summarized in Figure 1. While these results were very encouraging signs that soot emissions could be reduced by modifying the diesel fuel composition, the phenomenological results could not be explained in fundamental terms. Subsequent experimental engine studies[4−11] have extended these results to other oxygenated species. In addition, Litzinger et al.[12,13] recently combined experimental and kinetic modeling analysis of the soot-reducing effects of oxygenated species (i.e., ethanol and dimethyl ether) on sooting laminar premixed and diffusion ethane-air and ethylene-air flames, and while these flames and fuel are quite distinct from diesel combustion, they provide valuable chemical insights into soot reduction chemistry. Renard et al.[14] carried out experimental studies of premixed ethene/oxygen/argon laminar flat flames at slightly sooting rich conditions and examined the effects of adding small amounts of the oxygenated hydrocarbon dimethoxy methane (DMM). They found that the addition of DMM reduced the levels of soot precursor species in their premixed system, and they also cited a number of unpublished reports in which DMM was found to reduce soot emissions from diesel engines.

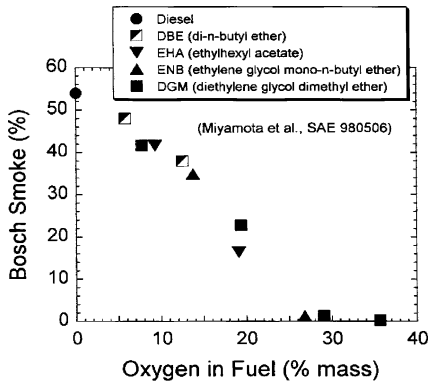

Figure 1. Variations in experimentally measured soot emissions from a diesel engine[3] with oxygenated species additions.

The present work uses detailed chemical kinetic modeling to address sooting reduction in diesel engines by oxygenated additives and explain the behavior in fundamental terms. A basic understanding from this kinetic modeling may suggest other mechanisms for modifying sooting processes. The same analysis can make it possible to evaluate the soot-reducing potential of other oxygenated species, including commercially important biodiesel fuels.

Modeling Approach

Our kinetic modeling study is constructed upon a conceptual model for diesel combustion developed by Dec and his colleagues, who used an extensive set of laser-based diagnostic techniques[15−21] to describe the major chemical and physical

† Part of the special issue "David M. Golden Festschrift".

* To whom correspondence should be addressed. E-mail: westbrook1@llnl.gov.

‡ National University of Ireland, Galway, Ireland.

10.1021/jp056362g CCC: $33.50
Published on Web 03/29/2006

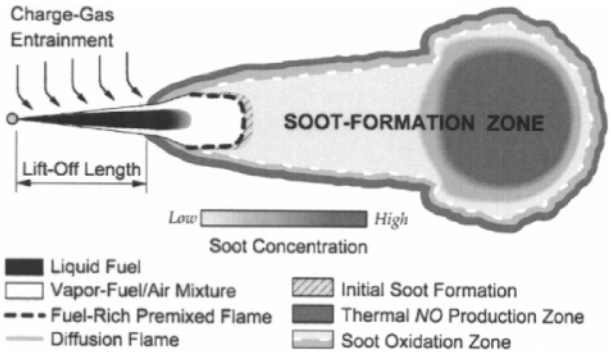

Figure 2. Phenomenological description of the major features of diesel combustion from experimental studies of Dec.[15]

steps that occur during diesel combustion. According to this picture, shown in Figure 2, shortly before the end of the compression stroke of the piston, diesel fuel is injected in a number of liquid jets into hot, highly compressed air and residual combustion products in the combustion chamber. Each fuel jet vaporizes rapidly and entrains and mixes with hot air. The hot air steadily raises the temperature of the vaporized fuel while simultaneously increasing the ratio of air to fuel. This mixture eventually ignites in the gas phase while still under quite fuel-rich conditions, with a local equivalence ratio ϕ of about 3 (i.e., three times as much fuel as could be fully oxidized by the air mixed locally with the fuel). The location of this fuel-rich premixed ignition is identified as the dashed curve in Figure 2.

The products of this ignition cannot be oxidized completely, due to the absence of sufficient oxygen. Therefore, these incompletely oxidized species such as CO, H_2, and small, intermediate hydrocarbon species including acetylene, ethene, propene, and others then react to produce soot[17−19] which is later consumed in a diffusion flame environment[19] farther downstream of the ignition region. The same unsaturated hydrocarbon species have been identified as major contributors to soot production in both diesel engines and laboratory flames.[21−32]

Our kinetic modeling approach is to compute an idealized rich, premixed ignition, using detailed chemical kinetic reaction mechanisms for the diesel fuel and any oxygenated additives. This ignition calculation is carried out under conditions of pressure, temperature, and fuel/air ratios that are characteristic of a diesel engine at the top of the piston stroke. The composition of the ignition products are then identified, and their relative sooting tendencies are evaluated.

To carry out these model calculations, we must make several important simplifications to this problem. Since we do not have kinetic reaction mechanisms for all of the hundreds or even thousands of species present in conventional diesel fuel, we use *n*-heptane as a convenient substitute or surrogate for diesel fuel, using a kinetic reaction mechanism we developed.[33] *N*-heptane has frequently been used as a diesel surrogate.[34−38]

The ignition properties of diesel fuel are described by its cetane rating in much the same way that the knocking behavior of gasoline in spark-ignition engines is characterized by its octane rating; *n*-heptane has a cetane rating of 56 that is typical of ordinary diesel fuels, and its rich ignition products include many of the species found to lead to soot production.

In addition, we do not directly simulate the mixing of the injected fuel and hot air, instead using the results of mixing experiments and other modeling studies as described by Naber and Siebers[39] as follows. The start of injection takes place about 10° before Top Dead Center (TDC, the point at which the piston reaches the most compressed point in its cycle) in Dec's

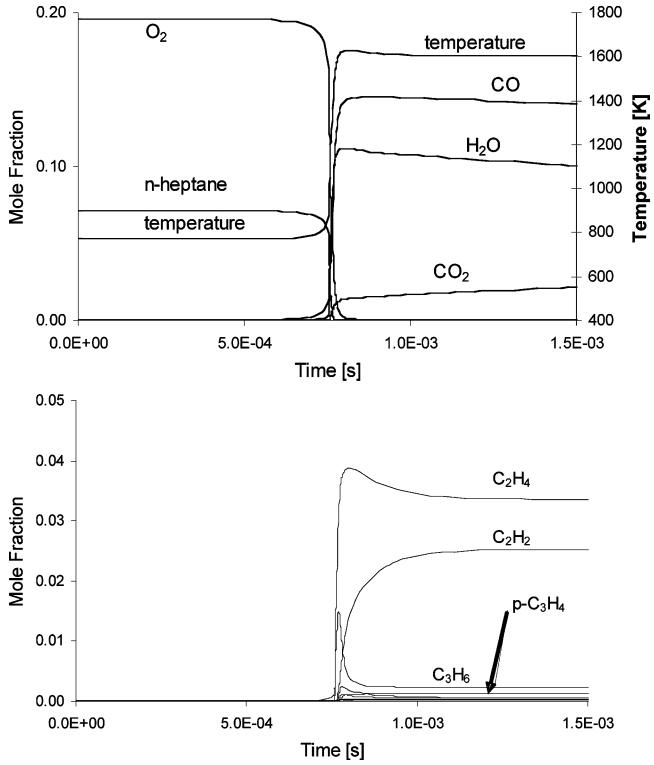

Figure 3. Computed temperature and major species mole fractions in the fuel-rich ignition of *n*-heptane/air at an equivalence ratio of 3, 10 MPa pressure, and initial temperature of 767 K.

engine,[15] so the compressed air already has a relatively high temperature and pressure. We use temperature-dependent specific heats for the reactants and air, as well as the heats of vaporization of the liquid fuel components, to mix cold fuel and hot air until the mixture reaches a temperature of about 770 K, where the kinetic model indicates that significant reaction begins to occur. At this point, the kinetic simulations begin. The fuel/air equivalence ratio is usually close to 3.0 at this point, although not every mixture will have exactly the same equivalence ratio, since the specific heats and heats of vaporization of *n*-heptane and each of the oxygenates we used are different. We have assumed that the combustion chamber pressure is 10 MPa at this point.

Once the ignition calculations begin, the simulations are performed in a constant pressure, spatially homogeneous environment, effectively decoupling the ignition process from the rest of the combustion chamber. In addition to the considerable simplification that these assumptions provide, these conditions are quite reasonable since the ignition of these fuel/air mixtures is quite rapid (<1 ms) in the diesel combustion chamber and there is little time for further exchange of heat or chemical species between the igniting mixture and the remainder of the combustion chamber.

In each model calculation, there is an initial induction period during which the temperature remains almost constant, chemical radical species are produced, and the reactant concentrations decrease very slowly. After this short time delay, a very rapid ignition occurs during which the reactants are completely consumed, the temperature increases from about 770 K to about 1600 K, and the products reach levels which remain nearly constant. This sequence is illustrated in Figure 3 for the case of neat *n*-heptane fuel, showing the major reactants and products, with the ignition occurring at about 0.75 ms. Note that, under these very rich conditions, the CO product concentration is much larger than that of CO_2.

TABLE 1: Species Present in the Ignition Products

	baseline case	with oxygenate	
species mole fraction	C_7H_{16}	C_7H_{16}/CH_3OH	C_7H_{16}/MB
temperature	1600 K	1750 K	1665 K
CO	0.140	0.133	0.152
CO_2	0.024	0.036	0.036
H_2	0.087	0.122	0.097
H_2O	0.100	0.119	0.106
CH_4	0.052	0.028	0.038
C_2H_4	0.034	0.013	0.022
C_2H_2	0.025	0.023	0.023
C_2H_6	0.002	0.0004	0.0011
PC_3H_4	0.0013	0.0005	0.0008
C_3H_6	0.002	0.0005	0.0011
C_4H_6	0.0006	0.0001	0.0003
N_2	0.532	0.524	0.522

The temperature and mole fractions of all of the species with values greater than 0.001 are summarized in Table 1. For the baseline calculation, the only major species not shown in Figure 3 are H_2 and H_2O, with product mole fractions of 0.087 and 0.100; H_2 plays a minor role in soot production and growth, and water plays virtually no role. The C_4 species with the highest mole fraction is 1,3-butadiene, which is shown in Table 1.

The key to this analysis is the identification of those species in the rich ignition products which enhance soot production and those which compete with soot production. We rely largely on the soot modeling work of Frenklach et al.,[22,23] which is based in turn on many careful and thorough experimental soot evolution studies, including particularly refs 24−30. The overall picture of soot kinetics that emerges from these studies is that small aromatic and polycyclic aromatic hydrocarbons (PAH) such as benzene, toluene, naphthalene, pyrene, and styrene are produced from small unsaturated hydrocarbons such as acetylene, ethene, propene, allene, propyne, and cyclopentadiene, as well as resonantly stabilized hydrocarbon radical species such as propargyl, allyl, methyl allyl, and cyclopentadienyl.[31] Subsequent reactions increase the size of the PAH species, leading eventually to visible soot, with acetylene being the most significant growth species.[23,25] Another key to understanding sooting chemistry is that the carbon atoms bonded to oxygen atoms in oxygenated species including CO and CO_2 do not become incorporated into soot.

There are two related methods to evaluate the relative sooting tendencies of rich ignition products under diesel conditions. The first method couples the PAH production mechanism of Appel, Bockhorn, and Frenklach[23] together with our own mechanisms for the fuel mixture ignition to predict levels of PAH species. This coupled mechanism approach has previously been employed successfully to predict soot production.[11−14] The second approach has been simply to sum all of the concentrations of known soot precursors (i.e., acetylene, benzene, ethene, toluene, propene, and other unsaturated stable and resonantly stabilized hydrocarbons) that remain following the rich ignition event.[9,10,21] Neither of these approaches can provide accurate values of total soot produced, and a great deal more experimental and kinetic modeling analyses will be necessary to provide this capability, but these techniques provide realistic estimates of *relative* soot production, which is suitable for the present study of soot reduction kinetics. In this work, we report results calculated using this second approach.

Kinetic Reaction Mechanisms. As noted above, *n*-heptane is used as the surrogate for diesel fuel. The reaction mechanism for *n*-heptane[33] has been used widely in kinetic modeling studies, due in part to it being conveniently available on the web.[40] It includes more than 2400 elementary reactions with nearly 600 chemical species, including the low-temperature, alkyl peroxy submechanisms that provide early heat release and advance the timing of the eventual hot ignition.

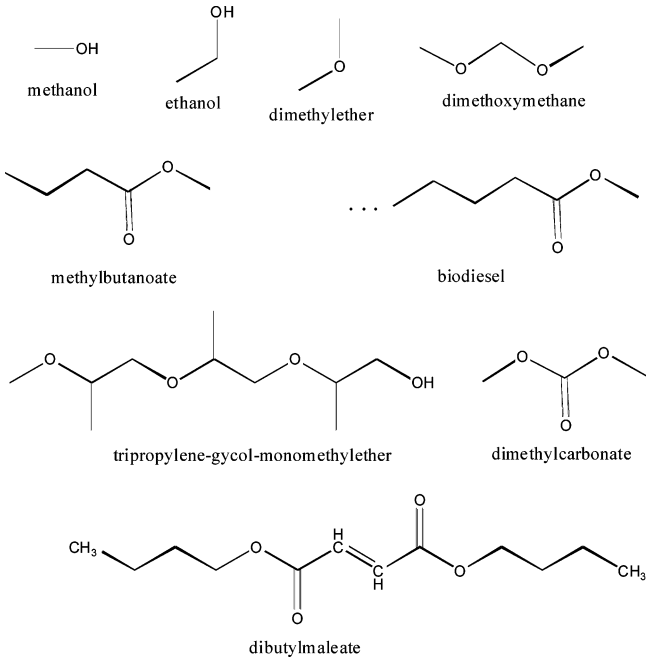

Figure 4. Chemical structures of oxygenated species used in model calculations.

Most of the oxygenates used in this study had detailed kinetic reaction mechanisms already available which were used without further modification, including mechanisms for methanol,[41] ethanol,[42] dimethyl ether,[43−46] dimethyl carbonate,[47] and methyl butanoate.[48] However, new kinetic mechanisms were also developed for dimethoxy methane (DMM) and two other considerably more complex oxygenated species, tripropylene glycol methyl ether (TPGME), and dibutyl maleate (DBM). Both TPGME and DBM were recommended[4] as oxygenated hydrocarbons with substantial O atom loading (four oxygen atoms per molecule) which have satisfactory fuel properties such as diesel fuel solubility and are relatively economical to produce. The structures of all of the oxygenates used in this study are summarized in Figure 4.

Methyl butanoate was selected for analysis as a convenient substitute for the very large methyl ester molecules that are typical of so-called biodiesel fuels. This similarity is shown in Figure 4, showing that both molecules have the same oxygenated section, but biodiesel molecules have a much larger hydrocarbon segment, often with as many as 16−18 C atoms. As described below, the computed results for the methyl ester structure were sufficiently interesting and potentially important that we chose to also consider the kinetics of dimethyl carbonate, also shown in Figure 4, which, along with DBM, also has an oxygenated structure similar to that of the biodiesel fuels.

Detailed chemical kinetic reaction mechanisms were developed for DMM, DBM, and TPGME. As in our previous mechanism developments,[47] thermodynamic parameters were estimated using quantum chemistry methods and group additivity.[49−51] For some species, the enthalpy of formation was computed using CBS-Q methods with geometries optimized at the B3LYP/6-31G9(d,p) level following Bozzelli,[52] and other details of the techniques are described by Glaude et al.[47] In the case of DMM, a low-temperature submechanism was developed and added to a previously existing high-temperature mechanism from Daly et al.[53] Low-temperature submechanisms were not

included for the large oxygenated species TPGME or DBM; no low-temperature oxidation experiments have been reported for the oxidation of these species on which to base a reaction submechanism, and the results computed in the present study for both DME and DMM, which included low-temperature kinetic reaction paths, were found to be insensitive to the low-temperature kinetics. This is primarily a result of the fact that our computations routinely began at temperatures close to 800 K, above the range of most alkylperoxy radical isomerization reaction pathways, so low-temperature reactions should not be expected to be significant. As a result, we do not believe such reactions to contribute to our results in the cases of DBM or TPGME. All of these kinetic mechanisms are available on our web page;[40] listings in Chemkin format for all the calculations reported here, and additional details for the mechanisms of TPGME and DBM, with literature sources for all the species-specific reaction rates for these new fuels are provided as Supporting Information.

Computational Results

The baseline calculation for this study is the ignition of *n*-heptane and air, at an equivalence ratio of about 3.0, a fixed pressure of 10 MPa, and an initial temperature of 767 K, as described above and shown in Figure 3. Because this mixture is so fuel-rich, the product temperature of 1600 K is considerably below the adiabatic flame temperature (>2200 K) of the corresponding stoichiometric *n*-heptane/air mixture. It is important to note that all of the initial fuel and O_2 are entirely consumed. The major soot precursors, ethene, acetylene, propyne, and propene for this baseline mixture are shown in Figure 3. No other soot precursor species are present in the rich ignition products at any significant level; the soot precursor species with the next highest concentrations are allene and 1,3-butadiene at levels nearly an order of magnitude less than propyne and propene in this baseline case with *n*-heptane as the fuel. Of course, other intermediate species, especially radical species present in these residuals, will contribute to soot production following the rich ignition, but their concentrations are much too low to contribute to the totals shown in Figure 3. Such radicals facilitate kinetically the subsequent formation of soot, but the basic soot building blocks are the precursors shown in Figure 3. The total amount of carbon present in these unsaturated soot precursor products comprises approximately 44% of the total carbon in the initial fuel. These products then produce small aromatic species, including benzene, toluene, naphthalene, and styrene, and eventually soot, as described by Appel et al.[23]

We repeated this baseline calculation, gradually replacing *n*-heptane fuel with amounts of the oxygenated hydrocarbon species shown in Figure 4. For each of these oxygenated species, as *n*-heptane is replaced by the oxygenate, the fraction of carbon remaining in the form of soot precursors in the rich ignition products decreases, being replaced by increased levels of CO and CO_2. Product concentrations for a fuel mixture with a nearly equimolar mixture of *n*-heptane and methanol (0.4 *n*-heptane + 0.6 methanol) are shown in Figure 5, and the product mole fractions of the major species are summarized in Table 1. The ignition time is slightly longer than the baseline, but the overall chemical features of the two ignitions are quite similar. However, the CO_2/CO ratio increases in the products, and the total carbon in the unsaturated species in the products is much lower. The temperature in the oxygenated case is 1750 K, higher than the 1600 K in the baseline case, because the increased oxygen content has brought the mixture closer to stoichiometric. Ethene is much lower while acetylene is only slightly reduced,

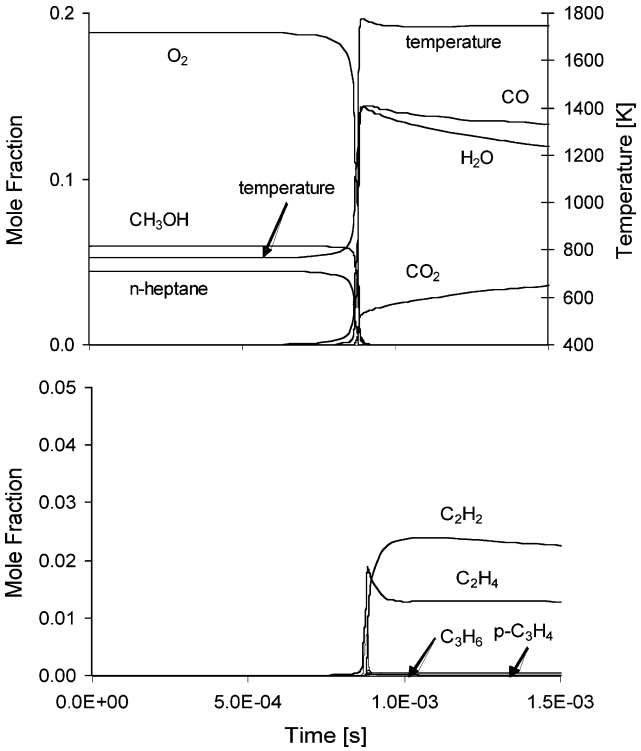

Figure 5. Computed major species mole fractions in the fuel-rich ignition of *n*-heptane/methanol/air at 10 MPa pressure and an initial temperature of 767 K.

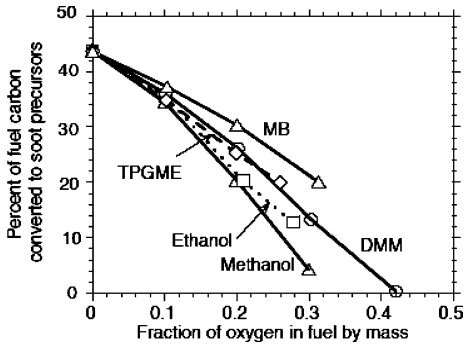

Figure 6. Computed reductions in soot precursor concentrations with the addition of selected oxygenated species: MB, methyl butanoate; DMM, dimethoxy methane; TPGME, tripropylene glycol methyl ether.

and the overall reduction in this carbon soot precursor pool is from 44% in the baseline case to about 28% in the mixed fuel case. The fraction of oxygen in the two-component fuel is 15%.

Further replacement of *n*-heptane by methanol further reduces the soot precursors in these products, until the soot precursor levels become very small when oxygen reaches about 30% of the total mass of the mixed fuel of *n*-heptane and methanol, as shown in Figure 6. At this point, the fuel consists of 17% *n*-heptane and 83% methanol on a molar basis or

$$\text{Fuel composition at soot elimination} = 1C_7H_{16} + 5CH_3OH$$

Note that, in this fuel mixture, 42% (i.e., 5/12) of the initial carbon atoms are already bonded to oxygen in the oxygenate (i.e., methanol) molecules. Under these conditions, it is clearly inappropriate to refer to the methanol as an "additive", since it is the major component in the fuel and more than 60% of the total fuel mass. Further insight is provided by noting that, since all of these mixtures also include nearly the same amount of entrained air, the overall equivalence ratio, including the oxygen

atoms in the methanol, has been reduced from 3.0 to about 2.2 by the addition of this much methanol.

The influence of the mixture equivalence ratio at the time of rich ignition on sooting is complex. In the present analysis, the equivalence ratio at the time of ignition is varied primarily by inclusion of different amounts of oxygenated species. In contrast, Siebers and Higgins[54] systematically varied the amount of entrained air and therefore the equivalence ratio at the time of diesel ignition by varying the injection pressure of diesel fuel into a constant volume combustion bomb and the corresponding variation in flame lift-off length. Siebers and Higgins found the amount of soot production to be quite sensitive to the amount of entrained air. They also observed that soot production became negligible when enough air was entrained to produce a local equivalence ratio of approximately 2 at the time of ignition. A comparison of this result with the present kinetic modeling results shows that providing additional oxygen for the ignition, either through extra entrained air or through its presence within the fuel molecules, reduces the amount of carbon in those species available for producing soot.

We repeated the same series of rich ignition calculations using other oxygenated species including ethanol, dimethyl ether, dimethoxy methane, and methyl butanoate. These model calculations produced results very similar to those for methanol, and the resulting decreases in soot precursor concentrations in the ignition products are summarized in Figure 6. It is important to note that all of these nearly straight lines are quite similar to the results from the experimental diesel engine studies summarized in Figure 1.

The first-order conclusion from Figure 6 is that all of the oxygenates included reduced the levels of soot precursor species at approximately the same rate. Some of the rather small differences in the curves shown in Figure 6 for the different additives can be attributed to uncertainties in the kinetic rates in the mechanisms, but other minor trends can be traced to differences in reaction pathways that occur for each oxygenate. By a rather small margin, methanol is the most effective additive in reducing soot precursor levels, and it should be noted that, since methanol reacts primarily to produce formaldehyde, methanol itself produces no hydrocarbon intermediates that promote soot precursor or soot production. Every carbon atom added to the mixture in the methanol molecule is already bonded to an O atom, and this bond is maintained all the way to CO_2 formation. In contrast, although ethanol combustion produces considerable amounts of the oxygenated intermediate species acetaldehyde, it also produces some ethene and some methyl radicals, both of which contribute to soot precursor production. Similarly, DMM primarily produces formaldehyde and methyl radicals (shown in more detail below), and this methyl radical can lead to ethene and acetylene via the methyl−methyl recombination reaction pathway. As discussed further below, TPGME also produces some soot precursor intermediates and some C−O bonded carbon during its consumption. In this manner, the detailed consumption pathways of the additive can contribute to soot precursor formation while simultaneously removing C atoms from the soot precursor pool, except in the case of methanol. These effects are different from those that limit the effectiveness of MB, which will be addressed below.

Several other features and limitations of Figure 6 should be noted. As already noted for the addition of methanol to the *n*-heptane fuel, a lot of additive is often needed to reach oxygen fractions as large as 20% or 30%. In some cases, these curves never reach a sufficiently high oxygen content to reach the *x*-axis. For example, if all of the *n*-heptane is replaced by TPGME, the resulting fuel has only about 32% oxygen by weight. Similarly, methyl butanoate (MB) has an overall composition of $C_5H_6O_2$ or about 33% oxygen by weight, so complete dilution of *n*-heptane by 100% MB will produce a fuel with 33% oxygen, which as seen in Figure 6 does not reduce the soot precursor levels to zero. DBM, which we will discuss below, is only 28% oxygen by weight, while dimethyl carbonate (DMC), another fuel discussed below, has about 53% oxygen, so the oxygen fractions available by dilution can vary significantly.

The reaction mechanisms for some of the oxygenates are somewhat uncertain since they have not been tested or validated due to the lack of available experimental data under controlled conditions. It is also important to remember that these computed results are extremely remote from an in-cylinder simulation, and therefore, the connection between them and expected engine soot production is very approximate. In some cases, only the trends should be credible. The highest confidence possible is that the slopes of all these curves are negative, so they all predict that the addition of oxygenates will in fact reduce soot production. Relative rates of soot reduction by different oxygenates have the next level of confidence, and specific amounts of oxygenates required to suppress sooting completely are the most speculative. The purpose of this computational study is to understand the kinetic reaction pathways and interpret those trends in which we are most confident, including the relative rates of soot suppression by different classes of additives.

The ultimate use of oxygenated compounds in diesel fuel may be limited to the addition of small fractions to reduce soot production slightly to satisfy emissions regulations or in coordination with combined soot and other emissions reduction strategies. In such cases, the only relevant part of Figure 6 would be the region describing small oxygen fractions, perhaps of only 1−5% oxygen.

The major soot precursors remaining in the ignition products of all of these mixtures are acetylene, ethene, propene, and other C_3 compounds including propargyl radicals (C_3H_3), as shown in Figures 3 and 5. Nearly all of the oxygen appears as CO and H_2O, with quite small amounts of CO_2. Water is produced via H atom abstraction reactions from the fuel by OH, and water production leads to most of the heat release leading to ignition. As the mass fraction of oxygen in the fuel mixture increases, a larger fraction of the total amount of carbon in the fuel is converted to CO and CO_2 and a smaller amount of carbon is present as soot precursors. When the PAH formation kinetic model of Appel et al.[23] is incorporated into our model calculations, concentrations of PAHs in the products are correspondingly reduced steadily as the oxygen content of the fuel increases, reaching near-zero levels when the oxygen content in the fuel reaches approximately 30%. This value for the oxygen content when the soot precursor level falls to zero is approximately the same as that shown in Figure 1 for the measured soot emissions from experimental diesel engines.

The same precursors and PAH species were produced in all of the modeling calculations carried out, although the amounts of these species decreased as oxygenate levels increased. This occurs because we used the same fuel for all of our calculations, and the intermediate species, particularly ethene and its most significant subsequent product acetylene, that we associate with soot production in Figures 3 and 5 are particularly strongly associated as those produced by *n*-heptane. For a different surrogate diesel fuel with different structure, other soot precursors could be produced; for example, with multiply branched hydrocarbons such as isooctane, we would expect little ethene

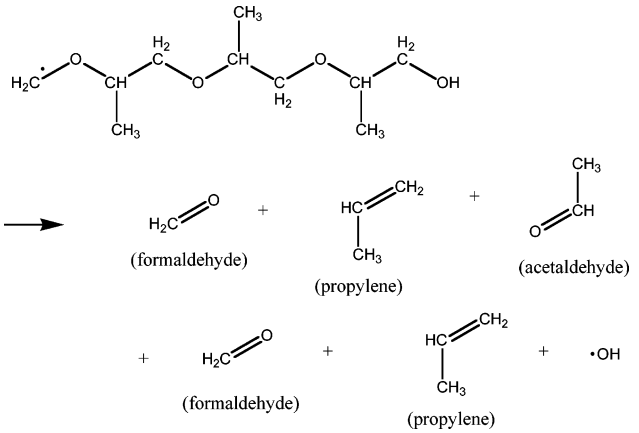

Figure 7. Schematic diagram of the overall products of consumption of TPGME.

but large fractions of isobutene and aromatic fuels are likely to produce another group of unsaturated small species as soot precursors. In each case, we would expect post-ignition levels of all soot precursors to decrease similarly as oxygenates are added to the fuel.

Careful examination of the kinetic pathways associated with the ignition of these oxygenates showed that nearly all of the oxygen atoms initially present in the oxygenates react directly to produce CO; the strong CO bond remains intact during the ignition, so the C atom in this bond never becomes available for soot production. When methanol is the oxygenate, it is consumed[41] primarily via a very linear reaction path

$$CH_3OH \rightarrow CH_2OH \rightarrow CH_2O \rightarrow HCO \rightarrow CO$$

In dimethoxy methane and dimethyl ether, each oxygen atom is initially bonded to two C atoms. During its combustion, one C−O bond is broken and the O atom remains bonded to another C atom. Specifically, in the case of DME, the dominant reaction pathway is H atom abstraction to produce methyl and formaldehyde

$$CH_3OCH_3 \rightarrow CH_2OCH_3 \rightarrow CH_2O + CH_3$$

which leaves the O atom bonded to one C atom. As in methanol oxidation, formaldehyde reacts directly via HCO to produce CO. Similarly, DMM reacts primarily by H atom abstraction

$$CH_3O(CH_2)OCH_3 \rightarrow CH_2O(CH_2)OCH_3 \rightarrow CH_2O + CH_2OCH_3$$

followed by

$$CH_2OCH_3 \rightarrow CH_2O + CH_3$$

with each O atom remaining bonded to one C atom, leading to CO formation.

The same analysis for TPGME is somewhat more complex, since the molecule is much larger and there are many possible H atoms that can be abstracted to initiate its oxidation. One of the eleven possible H atom abstraction steps can be used as an illustration as shown in Figure 7. In this case, one of the H atoms from the CH_3 group at the end of the molecule has been abstracted, leaving a large radical species that, under the present ignition conditions, decomposes rapidly via a series of β-scission paths. The ultimate set of products is shown as two formaldehyde molecules, two propylene molecules, one molecule of acetaldehyde, and an OH radical. In this example, three of the four O atoms in TPGME remain bonded to carbon atoms, and these carbon atoms are therefore eliminated from the pool of possible soot precursor species. When the same analysis is repeated for the other 10 radicals that can be produced from H atom abstraction from TPGME, a very similar group of products is created, in which one or two propylene molecules are produced and either three or four O atoms remain bonded to C atoms. None of these reaction paths produces two O atoms bonded to a single C atom, so the overall result is an efficient usage of the O atoms initially present in the TPGME in preventing those C atoms from contributing to the pool of available soot precursor species. The important feature is the distribution of O atoms in the TPGME molecule, so that each O atom leads to a CO molecule in the ignition products.

For all of the oxygenates above, almost every O atom in the oxygenate removes one C atom from the pool of species that can produce soot. In each case, the O atom is initially bound to a C atom and this bond is not subsequently broken. These oxygenated species displace C atoms in the diesel fuel with C atoms that are bonded to O atoms. This displacement exchanges C atoms that *can* produce soot with C atoms that, since they are bonded to O atoms, *cannot* contribute to soot production. Each of these oxygenated species is equally effective, per O atom in the additive, because each O atom removes one C atom from the soot-producing pool of species. The specific structure of the oxygenate has little impact on this process, provided that the structure retains the ability of each O atom to remove one C atom from the soot-producing pool of species.

All of the oxygenates shown in Figure 6 reduce the levels of soot precursors and at sufficiently high concentrations will eliminate soot emissions. From the results in Figure 6, most of these oxygenates are quite similar in their ability to reduce soot emissions. However, the curve for methyl butanoate (MB) suggests that its inhibiting power is slightly less than the other oxygenates in its ability to reduce soot precursor formation. This result could be due to errors in the development of the kinetic mechanism, for which very little experimental data are available for mechanism validation. MB had been chosen for attention because of its similarity to biodiesel fuels, so it is important to determine if this trend is significant and reflects real kinetic features, and if so, what kinetic factors are responsible for the computed behavior.

Methyl Ester Structures. There is considerable interest in the use of so-called biodiesel fuels, fuels derived from vegetable oils which have combustion properties similar to conventional diesel fuels. Such fuels are attractive since they represent a type of renewable fuel, and the fact that they include oxygen atoms gives them the potential to also reduce soot emissions when used in diesel fuels. Biodiesel fuels are usually produced from vegetable oils by esterification, which results in a characteristic structure with two O atoms located at the end of a long hydrocarbon chain. For most vegetable oils of interest,[55] the hydrocarbon chain contains 16 to 20 carbon atoms which can include several unsaturated segments, with a characteristic methyl ester group at one end shown in Figure 4.

We selected MB for kinetic modeling study to reduce the computational complexity of actual biodiesel fuels, making it possible to investigate the features of the methyl ester group without the computational complexity of the much larger hydrocarbon group.

As shown in Figure 4, the methyl ester group has two O atoms which are both bonded to a single C atom. The double C═O bond is very difficult to break, and the important question is

whether the other O atom remains bonded to the same C atom. The MB molecule

$$CH_3{-}CH_2{-}CH_2{-}(CO){-}O{-}CH_3$$

which replaces the long $C_{16}{-}C_{18}$ hydrocarbon chain typical of most biodiesel fuels with a short *n*-propyl radical is not consumed by thermal decomposition to any appreciable degree. Instead, it is consumed primarily by abstraction of H atoms by OH and H radicals, and the weakest C−H bonds are at the CH_2 groups in the hydrocarbon segment. When H abstraction produces

$$CH_3{-}CH{-}CH_2{-}(CO){-}O{-}CH_3$$

then β-scission leads to propene and the methoxy formyl radical

$$C_3H_6 + (CO){-}O{-}CH_3$$

As discussed below, the methoxy formyl radical then decomposes primarily to $CO_2 + CH_3$. When the H atom abstraction from MB produces

$$CH_3{-}CH_2{-}CH{-}(CO){-}O{-}CH_3$$

this radical decomposes to produce

$$CH_3{-}CH_2{-}CH{=}(CO) + CH_3O$$

leaving the O atoms bonded to different C atoms.

This analysis can be extended to describe larger methyl esters that are characteristic of realistic biodiesel fuels. If such molecules were completely saturated, with larger *n*-alkyl chains replacing the *n*-propyl group in MB, then H atom abstraction in the *n*-alkyl group, followed by β-scission of the resulting radical, would be expected to produce CO_2 and CH_3O in approximately equal amounts, exactly following the analysis above for MB. Considerable amounts of cross-linking and unsaturated portions are observed in the hydrocarbon portion of most bioderived methyl esters,[55] so the kinetic analysis is more complicated, and each biodiesel fuel is slightly different, but overall one would expect approximately the same mixture of CO and CO_2 to be produced from most biodiesel components.

We found that during combustion of the MB, approximately half of the reaction pathways resulted in both O atoms remaining bonded to the single C atom. As a result, CO_2 was produced directly and the two O atoms together removed only one C atom from the pool of reactive hydrocarbons that could produce soot. Computed results for the major species mole fractions are shown in Figure 8, which should be compared with the baseline case in Figure 3 and the nearly equimolar mixture of *n*-heptane and methanol shown in Figure 5. The exact mole fraction values are included in Table 1. For comparison, the initial fuel mixture in the two oxygenated cases with methanol and MB both contain 15% oxygen by mass. In the *n*-heptane/MB ignition, nearly all of the soot precursor and other products of the rich, premixed ignition reached final levels intermediate between the baseline and methanol additive cases and even the final temperature of 1665 K lies between the 1600 K of Figure 3 and the 1750 K of Figure 5. The final level of acetylene appears to be almost exactly the same in all three cases, but the reduction in ethene when MB is included is significantly less than when methanol is the oxygenated additive. It is clear that MB addition to the fuel enhances oxidation of the fuel and reduces the total level of soot precursors relative to the baseline without the oxygenate,

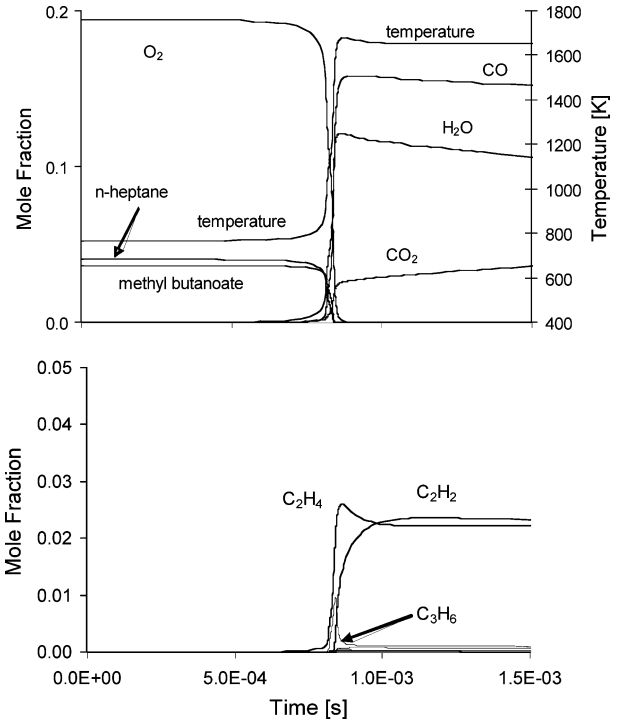

Figure 8. Computed major species mole fractions in the fuel-rich ignition of equimolar *n*-heptane/methyl butanoate/air at 10 MPa pressure and an initial temperature of 767 K.

but its effectiveness is still considerably less than what is observed when methanol is the additive.

In the details of the kinetic results, it is evident that the MB molecule is large enough to permit considerable amounts of low-temperature, alkylperoxy radical reaction processes at low temperatures. While temperatures are still below 1000 K, alkylperoxy radicals of the C_2, C_3, C_4, and C_7 species as well as HO_2 all react with the alkyl and alkylperoxy radicals produced by H atom abstraction from MB, and these radical reaction pathways produce considerable amounts of CO, explaining the calculation of higher CO levels in the *n*-heptane/MB fueled ignition, than in the case with methanol addition. In contrast, the much smaller methanol molecule involves little or no alkylperoxy radical reaction activity. However, the methyl ester structure of MB also leads to early production of CO_2 directly from MB, following H atom abstractions and decomposition of the resulting radicals as described above. As a result, these oxygen atoms are not available to assist in oxidizing the unsaturated hydrocarbon fragments, especially the acetylene and ethene, that produce soot following the ignition. While the overall reaction pathways for MB are quite complex at temperatures below 1000 K, the very simple mechanism outlined above becomes the dominant route for temperatures above 1000 K and both regimes produce CO_2 directly via the methoxy formyl decomposition reaction.

To examine this effect in greater detail, two additional oxygenated species were selected for further consideration, including dimethyl carbonate (DMC) and a larger species, dibutyl maleate (DBM), which had been selected by the same committee that had recommended TPGME for further study.[4] These structures are shown in Figure 4; both DBM and DMC are characterized by variations of the same ester structure as in MB. DMC was selected for two reasons; first, its high weight fraction of oxygen offers the possibility that it could have a strong soot inhibition effect on diesel combustion, and second, it provides a relatively clear way to examine the role of the

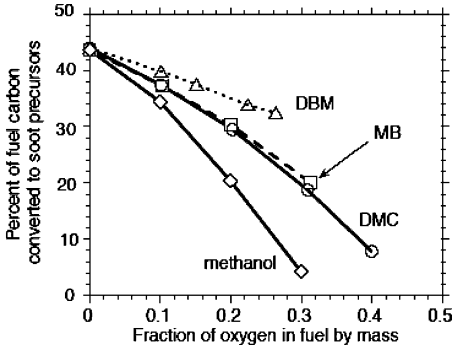

Figure 9. Computed reductions in soot precursor concentrations with the addition of an oxygenated species containing ester structure. MB is methyl butanoate, DMC is dimethyl carbonate, and DBM is dibutyl maleate, all shown structurally in Figure 4.

ester group in determining the kinetic fate of oxygen atoms in these oxygenated species. DBM was included because it was a more realistic practical diesel fuel component which had the same ester structure as MB and DMC but had a higher O atom content than the other oxygenates with the same structure.

In Figure 9, the relative effectiveness of these new oxygenated species on soot precursor reduction is summarized, together with the previous results for the cases with methanol and methyl butanoate as the oxygenates. These results show that all three oxygenates that have the characteristic ester group are less effective at reducing soot precursor levels than the oxygenates without the ester structure, on the basis of effect per unit oxygen atom in the fuel. The DBM is even less effective than methyl butanoate or dimethyl carbonate. In each of these cases, kinetic modeling shows that the particular locations and bond structures involving the O atoms lead to a considerable fraction of direct CO_2 formation from the oxygenate. This means that not every O atom in these compounds is able to eliminate a carbon atom from the soot precursor pool, resulting in a higher fraction of the remaining carbon atoms available to produce soot.

Combustion of these oxygenates (i.e., those containing the ester group) produces considerable amounts of the alkoxy formyl radical, (CO)−O−R, where R is an alkyl radical. In the case of DMC as the oxygenated species, in which R is the methyl radical, approximately 78% of the methoxy formyl radical decomposes to produce CO_2, with only 22% producing CO + CH_3O. In the case of DBM as the oxygenated species, nearly 90% of the analogous *n*-butoxy formyl radical produces CO_2. Glaude et al.,[47] McCunn et al.,[56] and Good and Francisco[57] have examined the methoxy formyl decomposition reaction, using CBS-Q and CCSD(T) methods at the B3LYP level, and all three studies agreed that the energy barrier to the CH_3 + CO_2 product channel is about 14.7 kcal/mol, while the barrier to the CH_3O + CO products is more than 22 kcal/mol, explaining why the CO_2 channel would be expected to dominate.

Discussion

Reduction of soot production by oxygenated species is a recent development, and relatively few experimental tests have appeared to date that can be used for confirmation of the mechanism presented here. On the basis of preliminary model predictions by the present authors, Buchholz et al.[10] used radiocarbon labeling of different C atoms in DBM to show experimentally that a significant fraction of the O atoms in DBM were converted directly into CO_2. They selectively labeled the three distinct carbon atoms shown in Figure 10 in successive experiments and used accelerator mass spectrometry (AMS) to detect ^{14}C in the CO_2 exhaust gases, in the soot that was

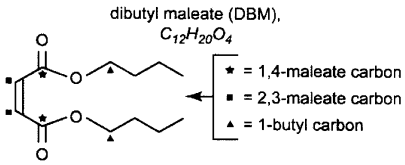

Figure 10. Schematic diagram of DBM, showing sites where C atoms were labeled with ^{14}C for accelerator mass spectroscopy.

collected, and in the surface deposits that were produced. Their analysis showed that the bonds between the 1-butyl groups and the adjacent O atoms were broken approximately 90% of the time and that the C atoms bonded to the two O atoms in DBM remained bonded through the rich ignition period, resulting in the direct production of CO_2.

Szybist and Boehman[58] have carried out compression-ignition studies in a CFR test engine, using as fuels both *n*-heptane and methyl decanoate, a monomethyl ester with a saturated, straight-chain alkyl radical with 10 carbon atoms. Their experiments measured heat release rates, gas temperatures, and exhaust gas composition using FTIR spectroscopy over a range of compression ratios leading to actual ignition. One important observation of their study was the production of CO_2 at very early stages of combustion associated with fuel decomposition, before any significant heat release had occurred. Early production of CO_2 was observed only when the fuel was methyl decanoate, and no corresponding CO_2 production was observed when the fuel was *n*-heptane. Their conclusion was that the CO_2 was a direct product of the methyl ester group in their methyl decanoate, consistent with the present kinetic modeling analysis.

Mueller et al.[9] directly compared the soot reduction effectiveness of DBM and TPGME in a diesel engine and in a constant volume combustion bomb. They found, in both experimental configurations, that TPGME was significantly more effective than DBM in reducing soot levels, which were measured using spatially integrated natural luminosity and line-of-sight laser extinction techniques. Experimental engine studies by Zannis et al.[60] also found that different oxygenated species structures produced different soot reduction efficiencies. The results of all of these experimental engine studies are consistent with the present description of how O atoms in the oxygenated species are used to suppress soot production.

The most obvious test of the present mechanism is that it predicts accurately the rate of soot suppression as the oxygen level in the fuel increases and the oxygen levels required to eliminate soot entirely. This is shown by comparing the experimental results in Figure 1 and the modeling predictions from Figure 6. Although this is an integrated result, it also is a widely observed phenomenon and the fact that the same behavior is observed for so many oxygenated fuel components and that the model reproduces those observations as well makes this a convincing test of the model.

We calculated the chemical equilibrium compositions for the mixtures summarized in Figures 3 and 5, with *n*-heptane and an *n*-heptane/methanol mixture as the fuels. We found that the major equilibrium components in each case consisted of CO, H_2 and CH_4, in addition to the N_2 present in the air. The other species in Figures 3 and 5, including H_2O, CO_2, C_2H_2, and C_2H_4 all are present in the equilibrium mixtures at levels of less than 1% mole fraction, indicating that the products computed kinetically are far from equilibrium. The product compositions in Figures 3 and 5 therefore represent an arrested kinetic process that had been proceeding to oxidation products. This permits us to summarize the evolution of the reactants through the ignition period.

Stoichiometric oxidation of *n*-heptane[33] occurs primarily by means of H atom abstraction, followed by decomposition of the resulting heptyl radicals; the principal next product is ethene as the long *n*-alkane chain is chopped into C_2H_4 blocks. Ethene is consumed by radicals to produce vinyl radicals (C_2H_3) which then decompose to produce acetylene. Subsequent oxidation of acetylene leads to CO and CO_2. Methane, a major component in the equilibrium calculations, is produced kinetically by H atom abstraction from the fuel by CH_3 radicals and very little of this occurs in these transient simulations. In the diesel-rich ignition calculations, it is clear that the computed reactions were proceeding normally toward combustion products when the limitations of the very fuel-rich environment quenched or interrupted the process. Because the rich conditions provide less heat release than stoichiometric conditions, the system cannot produce enough radicals to complete the oxidation process. Those radicals that are produced convert as much ethene as possible to acetylene, but it is clear from Figure 3 that this conversion is far from complete. OH radicals convert CO to CO_2 and produce H_2O from H atom abstraction reactions with the fuel, producing far more CO_2 and H_2O than is present at equilibrium conditions at these temperatures.

Kinetic production of superequilibrium CO_2 levels is a very important feature of this rich ignition and the production of soot in the diesel. At these rich conditions, the equilibrium composition contains none of the species normally associated with aromatic formation reaction pathways and soot production, particularly very low levels of ethene and acetylene. At equilibrium, all of the available O atoms are present in the form of CO. However, during the kinetically controlled ignition, the OH radicals that might have facilitated the equilibrium have instead oxidized CO to CO_2 and produced H_2O. The remaining C and H have no way to avoid remaining in the form of soot precursors, because the kinetic system has achieved a composition that is locally stable although far from true equilibrium. When O atoms in the oxygenated additive produce CO_2 immediately, because of the unfortunate placement of O atoms within those molecules, the imbalance toward CO_2 in the products is even more pronounced and the kinetic system remains far from the equilibrium that otherwise would have limited sooting.

When the oxygenate, methanol in this example, is added, some additional radicals are produced because the overall mixture, including the oxygenate, is slightly less rich (or closer to stoichiometric). The enhanced radical population converts more ethene to acetylene and more CO to CO_2, both of which are reflected in the comparisons between Figures 3 and 5. In addition, there is less ethene to convert to acetylene, since a great deal of the *n*-heptane has been displaced by methanol. As more oxygenate is added and the overall mixture becomes less fuel-rich, the steadily increasing radical pool is able to convert more intermediate species, particularly those which contribute to soot production, to nonsooting products. Eventually, as the overall equivalence ratio reaches 2.0, there are enough radical species to consume the ethene as well as the subsequent intermediate acetylene.

This analysis suggests how soot suppression is accomplished for the cases in which extra air is entrained.[54] Entrainment provides additional molecular oxygen, which reacts rapidly with radical species such as vinyl and produces HO_2 and OH radicals which then abstract H atoms from the fuel or react further with unsaturated species. Thus, oxidation of the fuel and particularly the soot precursor intermediates can proceed further with the addition of more oxygen and leave fewer species that produce soot. Increasing O_2 by air entrainment and the addition of oxygenates activate reaction pathways that advance the kinetic system toward final products and reduce the concentrations of those intermediates which lead to soot production. The details of the two reaction pathways are different, but the result is the same.

Both techniques, displacement of purely hydrocarbon fuel with oxygenates and dilution of the very rich fuel/air mixture with further air, could be characterized as simply changing the combustion equivalence ratio closer to stoichiometric, which would reduce sooting in a very intuitional way. However, the present analysis is intended to demonstrate that not all of the additional oxygen (and the associated change in equivalence ratio) is effective in reducing the production of soot when the dynamic nature of soot production is examined in kinetic detail.

The present analysis also suggests that different fuels will each have their own characteristic types of intermediate products with their own sooting properties. The present analysis has used *n*-heptane as the surrogate for diesel fuel, and the resulting soot precursors are predominantly ethene and its product acetylene. Branched alkanes will produce unsaturated intermediates that contain more branched species than in the present simulations, such as isobutene, in addition to acetylene and ethene. Cyclic alkanes and alkenes, and aromatic fuels, will each produce soot precursor species that are characteristic intermediate products of their oxygen-deprived or fuel-rich ignition. This provides the system "memory" of its original composition so the sooting tendencies and perhaps the morphology of the soot produced by different original fuels will vary as the distribution of the ignition products varies.

A particularly important subject for future study is the role of aromatic hydrocarbons in the fuel on the fuel-rich diesel ignition and the production of soot precursors. The soot modeling work of Frenklach,[22,23] as well as a large body of experimental work, has established that production of aromatic and polycyclic aromatic species is a major step toward soot production and the production of specific precursors to aromatic species formation has been a central element in the present study. As shown in Figures 3 and 5, our kinetic model predicts that all of the original fuel is consumed during the rich ignition, but a similar simulation of fuel-rich ignition of aromatic fuels under diesel conditions has not yet been addressed. Since the specific hydrocarbon fragments in the ignition products are influenced by the structure of the fuel, the composition of the soot precursors in the case of aromatic fuels may be quite different from the present species, and this will be addressed in future work.

Finally, it should be noted that the present analysis applies only to the case of premixed ignition. The same conclusions do not apply to nonpremixed systems such as diffusion flames, which are kinetically more complex than the present systems. For example, McEnally et al.[61,62] examined co-flowing methane *diffusion* flames to which a variety of butyl alcohols and alkyl ethers were added to the fuel, and in these cases, the oxygenated additive *increased* the production of soot. In direct contrast, the flame study of Renard et al.[14] examined rich *premixed* laminar flames in which the addition of DMM to an ethene/oxidizer mixture *reduced* the level of soot precursors. McNesby et al.[12] recently discussed soot formation in an opposed flow ethene/air flame, adding ethanol to the air stream and alternatively to the fuel stream, observing quite different responses of the sooting flame in these two cases. When they added the oxygenate to the fuel stream, soot production increased, and when the same oxygenate was added to the air stream, soot

production decreased. McNesby et al. observed that the addition of ethanol to the air side of the flame seemed to increase the premixed features of their flame, while the addition of ethanol to the fuel side of the flame interacted primarily with the fuel pyrolysis process.

The role of the oxygenated additive is seen to be quite different in these two regimes and emphasizes different reaction pathways. In this context, it is evident that ignition in the diesel engine is best characterized as a rich premixed environment and that nonpremixed flame studies do not address the same kind of soot production that occurs in the diesel engine. This might seem odd, since the common perception of diesel combustion is that it is a fundamentally diffusion-controlled combustion environment, but the observation that the addition of oxygenated species reduces soot production, consistent with experimental results from related premixed flames and in direct contradiction with nonpremixed flame studies, identifies soot production in diesel engines as a premixed combustion problem. The subsequent oxidation of the soot, which has been formed in the rich premixed environment, is certainly a diffusion-controlled process and confirms the overall diffusion character of diesel combustion, but the soot production is best characterized as a premixed phenomenon.

Summary

Diesel engine chemistry has been primarily an experimental subject, but the phenomenological model of Dec[15−21] has provided a framework within which focused computational studies can provide valuable insights. The present kinetic modeling analysis fits conveniently into Dec's framework, connecting the fuel vaporization and air entrainment processes with the soot growth period.

The key feature of the present study is that C−O moieties imbedded in oxygenated species displace carbon in the original diesel fuel; the C−O bond survives the fuel-rich ignition intact, so there is less carbon available to make soot in the oxygen-depleted post-ignition environment. Soot reduction has generally been measured experimentally as a reduction in soot emissions per O atom included in the reactant molecules. For some years, it was believed[3,54,59] that reduction of soot depended only on the amount of oxygen added to the diesel and was not affected by the specific oxygenate type. However, recent experimental and kinetic modeling analysis has shown[2,9−11,60] that there are some oxygenated species that use their oxygen atoms less efficiently than others. The present work attributes these effects to details in the structure of the oxygenated additive species, particularly in the case of ester species in which two O atoms are initially bonded to single C atoms. When these CO_2 moieties result in the direct production of CO_2 molecules, the oxygen initially present in the oxygenated hydrocarbon additives is therefore less efficient in eliminating C atoms from the product pool of species that can subsequently make soot.

Our modeling calculations show that soot formation is initiated by a fuel-rich premixed ignition of diesel fuel which is quenched due to lack of sufficient oxygen to burn the fuel completely. Oxygenated fuels reduce the production of soot precursor species during the rich ignition, a prediction that is consistent with trends observed experimentally in premixed flames but inconsistent with trends observed experimentally in nonpremixed flames in which oxygenated additives increase the concentrations of soot precursors and produce more soot than the associated nonpremixed flame without the oxygenated additive. These observations show that diesel ignition is an inherently premixed process, although subsequent soot burnout takes place in a diffusion flame.

Acknowledgment. The authors appreciate receiving information in advance of publication from Prof. Andre Boehman of The Pennsylvania State University and Prof. Laurie Butler of the University of Chicago. This work was supported by the U.S. Department of Energy, Office of FreedomCAR and Vehicle Technologies, and was performed under the auspices of the U.S. Department of Energy by the University of California, Lawrence Livermore National Laboratory under Contract No. W-7405-Eng-48.

Supporting Information Available: Listings in Chemkin format for all the calculations reported here and additional details for the mechanisms of TPGME and DBM, with literature sources for all the species-specific reaction rates for these new fuels are provided. This material is available free of charge via the Internet at http://pubs.acs.org.

References and Notes

(1) *Fed. Regist.* **2001**, *66* (12), 5005. Available from: http://www.epa.gov/fedrgstr/EPA-AIR/2001/January/Day-18-a01a.pdf.

(2) Ban, H.; Farrell, J. T.; Hotta, Y.; Nakakita, K.; Takasu, S.; Weissman, W. *Effect of Hydrocarbon Molecular Structure in Diesel Fuel on In-Cylinder Soot Formation and Exhaust Emissions*; Paper No. SAE 2003-01-1914; Society of Automotive Engineers, 2003.

(3) Miyamoto, N.; Ogawa, H.; Nurun, N. M.; Obata, K.; Arima, T. *Smokeless, Low NOx, High Thermal Efficiency, and Low Noise Diesel Combustion with Oxygenated Agents as Main Fuel*; Paper No. SAE 980506; Society of Automotive Engineers, 1998.

(4) Gonzalez, M. A.; Piel, W.; Asmus, T.; Clark, W.; Garbak, J.; Liney, E.; Natarajan, M.; Naegeli, D. W.; Yost, D.; Frame, E.; Wallace, J. P. Oxygenates Screening for Advanced Petroleum-Based Diesel Fuels: Part 2. The Effect of Oxygenate Blending Compounds on Exhaust Emissions. *SAE Trans.* **2001**, *101*, Paper No. SAE-2001-01-3632.

(5) Musculus, M. P.; Dec, J. E.; Tree, D. R. *Effects of Fuel Parameters and Diffusion Flame Lift-Off on Soot Formation in a Heavy-Duty Diesel Engine*; Paper No. SAE-2002-01-0889; Society of Automotive Engineers, 2002.

(6) Choi, C. Y.; Reitz, R. D. *Fuel* **1999**, *78*, 1303−1317.

(7) Mueller, C. J.; Martin, G. C. *Effects of Oxygenated Compounds on Combustion and Soot Evolution in a DI Diesel Engine: Broadband Natural Luminosity Imaging*; Paper No. SAE-2002-01-1631; Society of Automotive Engineers, 2002.

(8) Stoner, M.; Litzinger, T. A. *Effects of Structure and Boiling Point of Oxygenated Blending Compounds in Reducing Diesel Emissions*; Paper No. SAE-1999-01-1475; Society of Automotive Engineers, 1999.

(9) Mueller, C. J.; Pitz, W. J.; Pickett, L. M.; Martin, G. C.; Siebers, D. L.; Westbrook, C. K. *Effects of Oxygenates on Soot Processes in DI Diesel Engines: Experiments and Numerical Simulations*; Paper No. SAE 2003-01-1791; Society of Automotive Engineers, 2003.

(10) Buchholz, B. A.; Mueller, C. J.; Upatnieks, A.; Martin, G. C.; Pitz, W. J.; Westbrook, C. K. *Using Carbon-14 Isotope Tracing to Investigate Molecular Structure Effects on the Oxygenate Dibutyl Maleate on Soot Emissions from a DI Diesel Engine*; Paper No. SAE 2004-01-1849; Society of Automotive Engineers, 2004.

(11) Kitamura, T.; Ito, T.; Kitamura, Y.; Ueda, M.; Senda, J.; Fujimoto, H. *Soot Kinetic Modeling and Empirical Validation on Smokeless Diesel Combustion with Oxygenated Fuels*; Paper No. SAE 2003-01-1789; Society of Automotive Engineers, 2003.

(12) McNesby, K. L.; Miziolek, A. W.; Nguyen, T.; Delucia, F. C.; Skaggs, R. R.; Litzinger, T. A. *Combust. Flame* **2005**, *142*, 413−427.

(13) Wu, J.; Song, K. H.; Litzinger, T.; Lee, S.-Y.; Santoro, R.; Linevsky, M. *Combust. Flame*, **2006**, in press.

(14) Renard, C.; Van Tiggelen, P. J.; Vandooren, J. Effect of Dimethoxymethane Addition on the Experimental Structure of a Rich Ethylene/Oxygen/Argon Flame. *Proc. Combust. Inst.* **2002**, *29*, 1277−1284.

(15) Dec, J. E. A Conceptual Model of DI Diesel Combustion Based on Laser-Sheet Imaging; Paper No. SAE 970873; Society of Automotive Engineers, 1997.

(16) Dec, J. E.; Espey, C. Paper No. SAE 980147; Society of Automotive Engineers, 1998.

(17) Dec, J. E.; Espey, C. Ignition and Early Soot Formation in a DI Diesel Engine Using Multiple 2-D Imaging Diagnostics. *SAE Trans.* **1995**, *104*, (Sec. 3), 853−875, Paper No. SAE 950456.

(18) Dec, J. E. Soot Distribution in a DI Diesel Engine Using 2-D Imaging of Laser-Induced Incandescence, Elastic Scattering, and Flame Luminosity. *SAE Trans.* **1992**, *101* (Sec. 4), 101-112, Paper No. SAE-920115.

(19) Dec, J. E.; Espey, C. Soot and Fuel Distributions in a DI Diesel Engine Via 2-D Imaging. *SAE Trans.* **1992**, *101* (Sec. 4), 1642−1651, Paper No. SAE-922307.

(20) Espey, C.; Dec, J. E.; Litzinger, T. A.; Santavicca, D. A. "Quantitative 2-D Fuel Vapor Concentration Imaging in a Firing DI Diesel Engine Using Planar Laser-Induced Rayleigh Scattering. *SAE Trans.* **1994**, *103* (Sec. 3), 1145−1160, Paper No. SAE 940682.

(21) Flynn, P. F.; Durrett, R. P.; Hunter, G. L.; zur Loye, A. O.; Akinyemi, O. C.; Dec, J. E.; Westbrook, C. K. Diesel Combustion: An Integrated View Combining Laser Diagnostics, Chemical Kinetics, and Empirical Validation. *SAE Trans.* **1999**, *108* (Sec. 3), 587−600, Paper No. SAE-1999-01-0509.

(22) Frenklach, M.; Wang, H. *Proc. Combust. Inst.* **1990**, *23*, 1559−1566.

(23) Appel, J.; Bockhorn, H.; Frenklach, M. *Combust. Flame* **2000**, *121*, 122−136.

(24) Wagner, H. Gg. Soot Formation−An Overview. In *Particulate Carbon Formation During Combustion*; Siegla, D. C., Smith, G. W., Eds.; Plenum Press: New York, 1981; pp 1−29.

(25) Harris, S. J.; Weiner, A. M.; Blint, R. J.; Goldsmith, J. E. M. *Proc. Combust. Inst.* **1986**, *21*, 1033−1045.

(26) Richter, H.; Howard, J. B. *Prog. Energy Combust. Sci.* **2000**, *26*, 565−608.

(27) Bockhorn, H.; Fetting, F.; Wenz, H. W. *Ber. Bunsen-Ges. Phys. Chem.* **1983**, *87*, 1067−1073.

(28) Homann, K. H. *Combust. Flame* **1967**, *11*, 265−287.

(29) Haynes, B. S.; Wagner, H. Gg. *Prog. Energy Combust. Sci.* **1981**, *7*, 229−273.

(30) Marinov, N. M.; Pitz, W. J.; Westbrook, C. K.; Vincitore, A. M.; Castaldi, M. J.; Senkan, S. M.; Melius, C. F. *Combust. Flame* **1998**, *114*, 192−213.

(31) Miller, J. A.; Pilling, M. J.; Troe, J. *Proc. Combust. Inst.* **2005**, *30*, 43−88.

(32) McEnally, C. S.; Ciuparu, D. M.; Pfefferle, L. D. *Combust. Flame* **2003**, *134*, 339−353.

(33) Curran, H. J.; Gaffuri, P.; Pitz, W. J.; Westbrook, C. K. *Combust. Flame* **1998**, *114*, 149−177.

(34) Yelvington, P. E.; Rallo, M. B. I.; Liput, S.; Tester, J. W.; Green, W. H.; Yang, J. L. *Combust. Sci. Technol.* **2004**, *176*, 1243−1282.

(35) Hamosfakidis, V.; Reitz, R. D. *Combust. Flame* **2003**, *132*, 433−450.

(36) Samec, N.; Kegl, B.; Dibble, R. W. *Fuel* **2002**, *81*, 2035−2044.

(37) Lee, K.; Lee, C.; Ryu, J.; Kim, H. *Energy Fuels* **2005**, *19*, 393−402.

(38) Su, W. H.; Huang, H. Z. *Fuel* **2005**, *84*, 1029−1040.

(39) Naber, J. D.; Siebers, D. L. Effects of Gas Density and Vaporization on Penetration and Dispersion of Diesel Sprays; Paper No. SAE 960034; Society of Automotive Engineers, 1996.

(40) http://www-cms.llnl.gov/combustion/combustion2.html.

(41) Westbrook, C. K.; Dryer, F. L. *Combust. Sci. Technol.* **1979**, *20*, 125−140.

(42) Marinov, N. M. *Int. J. Chem. Kinet.* **1999**, *31*, 183−220.

(43) Curran, H. J.; Pitz, W. J.; Westbrook, C. K.; Dagaut, P.; Boettner, J. C.; Cathonnet, M. *Int. J. Chem. Kinet.* **1998**, *30*, 229−241.

(44) Fischer, S. L.; Dryer, F. L.; Curran, H. J. *Int. J. Chem. Kinet.* **2000**, *32*, 713−740.

(45) Curran, H. J.; Fischer, S. L.; Dryer, F. L. *Int. J. Chem. Kinet.* **2000**, *32*, 741−759.

(46) Zheng, X. L.; Lu, T. F.; Law, C. K.; Westbrook, C. K.; Curran, H. J. *Proc. Combust. Inst.* **2005**, *30*, 1101−1109.

(47) Glaude, P. A.; Pitz, W. J.; Thomson, M. J. *Proc. Combust. Inst.* **2005**, *30*, 1111−1118.

(48) Fisher, E. M.; Pitz, W. J.; Curran, H. J.; Westbrook, C. K. *Proc. Combust. Inst.* **2000**, *28*, 1579−1586.

(49) Benson, S. W. *Thermochemical Kinetics*, 2nd edition; John Wiley: New York, 1976.

(50) Ritter, E. R.; Bozzelli, J. W. *Int. J. Chem. Kinet. 23*, 767−778 1991.

(51) Lay, T.; Bozzelli, J. W.; Dean, A. M.; Ritter, E. R. *J. Phys. Chem.* **1995**, *99*, 14514−14527.

(52) Zhu, L.; Chen, C. J.; Bozzelli, J. W. J. *Phys. Chem. A* **2000**, *104*, 9197−9206.

(53) Daly, C. A.; Simmie, J. M.; Dagaut, P.; Cathonnet, M. *Combust. Flame* **2001**, *125*, 1106−1117.

(54) Siebers, D.; Higgins, B. Flame Lift-Off on Direct-Ignition Diesel Sprays Under Quiescent Conditions; Paper No. 2001-01-0530; Society of Automotive Engineers, 2001.

(55) Graboski, M. S.; McCormick, R. L. *Prog. Energy Combust. Sci.* **1998**, *24*, 125−164.

(56) McCunn, L. R.; Lau, K.-C.; Krisch, M. J.; Butler, L. J.; Tsung, J.-W.; Lin, J. J. *J. Phys. Chem. A* **2006**, *110*, 1625−1634.

(57) Good, D. A.; Francisco, J. S. *J. Phys. Chem. A* **2000**, *104*, 1171−1185.

(58) Szybist, J. P.; Boehman, A. L. Submitted for publication, 2005.

(59) Curran, H. J.; Fisher, E. M.; Glaude, P.-A.; N. M. Marinov, W. J.; Pitz, Westbrook, C. K.; Layton, D. W.; Flynn, P. F.; Durrett, R. P.; zur Loye, A. O.; Akenyemi, O. C.; Dryer, F. L. *Detailed Chemical Kinetic Modeling of Diesel Combustion with Oxygenated Fuels*; Paper No. SAE 2001-01-0097; Society of Automotive Engineers, 2001.

(60) Zannis, T. C.; Hountalas, D. T.; Kouremenos, D. A. *Experimental Investigation to Specify the Effect of Oxygenated Additive Content and Type on DI Diesel Engine Performance and Emissions*; Paper No. SAE 2004-01-0097; Society of Automotive Engineers, 2004.

(61) McEnally, C. S.; Pfefferle, L. D. Experimental Study of Fuel Decomposition and Hydrocarbon Growth Processes for Practical Fuel Components in Nonpremixed Flames: MTBE and Related Alkyl Ethers. *Int. J. Chem. Kinet.* **2004**, *36*, 345−358.

(62) McEnally, C. S.; Pfefferle, L. D. Fuel decomposition and hydrocarbon growth processes for oxygenated hydrocarbons: butyl alcohols. *Proc. Combust. Inst.* **2005**, *30*, 1363−1370.